Accepted for publication in the Astrophysical Journal

The bulk Lorentz factor crisis of TeV blazars : evidence for an inhomogeneous pileup energy distribution ?

Gilles Henri

Laboratoire d'Astrophysique de Grenoble, Université Joseph-Fourier, BP 53, F-38041 Grenoble, France

and

Ludovic Saugé

Institut de Physique Nucléaire de Lyon, UCBL/IN2P3-CNRS , 4, rue Enrico Fermi, F-69622, Villeurbanne cedex, France

Gilles.Henri@obs.ujf-grenoble.fr,l.sauge@ipnl.in2p3.fr

ABSTRACT

There is growing evidence that the estimations of the beaming Doppler factor in TeV BL Lac object based on the Self Synchrotron Compton (SSC) models are in strong disagreement with those deduced from the unification models between blazars and radio galaxies. When corrected from extragalactic absorption by the diffuse infrared background (DIrB), the SSC one-zone models require very high Lorentz factor (around 50) to avoid strong $\gamma - \gamma$ absorption. However, the statistics on beamed *vs.* unbeamed objects, as well as the luminosity contrast, favors much lower Lorentz factor of the order of 3. In this paper, we show that for the special case of Markarian 501, the need for very high Lorentz factor is unavoidable for all one-zone models where all photons are assumed to be produced at the same location at the same time. Models assuming a double structure with two different beaming patterns can partially solve the problem of luminosity contrast, but we point out that they are inconsistent with the statistics on the number of detected TeV sources. The only way to solve the issue is to consider inhomogeneous models, where low energy and high energy photons are not produced at the same place, allowing for much smaller Lorentz factors. It implies that the jet is stratified, but also that the particle energy distribution is close to a monoenergetic one, and that pair production is likely to be significant. The implications on relativistic jet physics and particle acceleration mechanism are discussed.

Subject headings: radiation mechanisms: non-thermal — gamma rays: theory — galaxies: active — galaxies: BL Lacertae objects: general — galaxies: jets

1. Introduction

It is now admitted that the blazar phenomenon is due to relativistic Doppler beaming of the non-thermal jet emission taking place in radio-loud Active Galactic Nuclei (AGN) where the jet axis is closely aligned with the observer's line of sight. They exhibit an important level of optical polarization, a flat radio spectrum, a strong variability in all frequency bands and a very broad spectral energy distribution (SED) ranging from the radio to the extreme gamma ray band. The SED consists typically in two broad components. In the so-called Synchrotron-Self-Compton process (SSC) model, the lowest energy hump is attributed to the synchrotron emission from relativistic electrons and/or positrons, and the highest one is attributed to the Inverse Compton (IC) process of the same charged particles onto the synchrotron photons and/or external photons. The blazar class of objects includes both the *Flat Spectrum Radio Quasars* (FSRQ) and the *BL Lac* sources (or Lacertids), depending respectively on the existence or the lack of detectable emission lines in their spectra. Following Chiaberge et al. (2000), one can define two classes of BL Lac objects (which are most probably two extreme cases in a continuous distribution) : the LBL or "red" BL Lac, for which the synchrotron component peaks in far IR to optical, and the IC component peaks in the MeV-GeV range, and the HBL or "blue" BL Lac, for which the synchrotron component peaks in the UV-X range, and the IC component peaks above 10 GeV. The most extreme objects up to now are those whose non thermal emission extends up to the TeV range, the so-called TeV blazars. The two main prototypes are Mrk 421 (Punch et al. 1992) and Mrk 501 (Quinn et al. 1996), two radio-loud AGN relatively close to us and roughly at the same distance, $z_s \approx 0.031$ and $z_s \approx 0.034$ respectively. Five other TeV detections have been repeatedly detected (1ES 1959+650, PKS 2155-304 (Aharonian et al. 2005a), 1ES 1426+428 and PKS 2005-489 (Aharonian et al. 2005b), and 1ES 2344+514 (Aharonian et al. 2004)). All of them are Lacertids, although it is not clear up to now whether only BL Lac objects do emit TeV radiation or if this is due to a selection effect. As a matter of fact, BL Lac objects appear to be much more numerous than quasars and the closest blazars all belong to this class. A high sensitivity threshold would strongly bias the detection toward the closest sources. Furthermore it is well-known that TeV photons are absorbed by the Diffuse Infra Red Background (DIrB) to create electron-positron pairs, and it is not obvious whether even the closest quasar, 3C 273 ($z_s \approx 0.158$) could be detected in the TeV range.

One-zone SSC models assume that highly relativistic particles are injected in a spherical zone, where they cool by emitting synchrotron radiation and by Inverse Compton process. The models require specifying the source radius, the magnetic field, as well as the density and the energy distribution of the emitting relativistic particles. The latter is most often assumed to be a power law or a broken power law (*e.g.* Marscher 1983; Tavecchio et al. 1998). It turns out however that the computation of emitted radiation is not compatible with the hypothesis of a static source, because in most cases the photon density would be so high that all TeV photons should be absorbed to form electron-positron pairs. Furthermore the time variability is so short (down to 15 minutes in some cases, Gaidos et al. (1996)) that it is incompatible with a spherical static source through the causality argument. This leads to assume that the source is moving with a relativistic bulk velocity $v = \beta c$. The effect of relativistic bulk motion is entirely described by the Doppler beaming factor $\delta = 1/\Gamma(1-\beta\mu)$, where $\Gamma = (1-\beta^2)^{-1/2}$ is the usual Lorentz factor and $\mu = \cos\theta$ is the cosine angle of the jet according to the observer's line of sight. The Doppler effect shifts all frequencies by a factor δ and all specific intensities by a factor δ^3. So the actual photon density in the jet frame is much lower than what would be deduced for a static source. The relativistic motion has been invoked for a long time (Rees 1966) to solve a similar issue for radio emission of quasars. Namely the brightness temperature is so high that, for a static sources, the relativistic leptons emitting synchrotron radiation should have cooled immediately through the so-called "Inverse Compton catastrophe" (Rees & Simon 1968). Again the relativistic motion can fix this issue, because the actual photon density in the jet frame is much lower when taking into account the Doppler amplification. This beautiful theoretical explanation has been later confirmed by the discovery of superluminal motion, which requires Lorentz factors at least as great as the observed apparent reduced velocity $\beta_{\rm app} = v_{\rm app}/c$ (for a review, see Zensus 1997).

For $\mu \gtrsim \beta$, corresponding to $\theta \lesssim 1/\Gamma$, one has $1 \leqslant \delta \leqslant 2\Gamma$, whereas $\delta \sim 1/\Gamma$ outside this interval. It means that for a few beamed Doppler sample of boosted sources, one expects a lot of unbeamed and not amplified counterparts. It is natural to think that the unbeamed counterparts of bright quasars are the weaker radio galaxies, whose jet is thought to make a larger angle with the line of sight. Particularly it has been proposed that the unbeamed counterparts of BL Lac object could be a sub class of radio galaxies, the so-called Fanaroff-Riley I (FRI) radio galaxies (Urry & Padovani 1995). These are characterized by a rather faint, weakly beamed, and core-brightened radio jet. Statistical studies of radio and X-ray AGN samples have confirmed the possibility of such an association. The inferred beaming factors seem to imply a rather modest value of the bulk Lorentz factor, of about 3. However, the modeling of SSC radiation by one zone models requires much higher values : following the authors, they range from 10 to 50 (Tavecchio et al. 1998; Konopelko et al. 2003; Saugé & Henri 2004). The highest value seems to be needed when one takes properly into account

the extragalactic absorption. The problem is further complicated by the absence of clear superluminal motion in TeV blazars, together with a rather modest brightness temperature, which implies also a low Lorentz/Doppler factor (Edwards & Piner 2002; Piner & Edwards 2004). All these contradictory facts lead to what we call here the "*Bulk Lorentz factor crisis of TeV blazars*".

The aim of this paper is first to ascertain this crisis. We will first show that all one-zone SSC models imply high Lorentz factors, only with the argument of $\gamma - \gamma$ absorption and discarding any variability argument. Then we will recall the arguments for low Lorentz factor, based on general geometric properties of the Doppler boosting. We will show that the explanations based on two different structures, with a possible deceleration of a fast spine responsible for TeV emission, are not satisfactory concerning the statistics of TeV blazars. We argue that the best solution is to admit the low Lorentz factor constraint, abandoning the one-zone assumption. We will show that this conclusion has important consequences regarding the jet physics and the particle acceleration mechanism.

2. The case for high Lorentz factor

In the following, we will develop the need for high Lorentz factors for one-zone models, with the fewest theoretical assumptions and relying only on observational data. We will only assume that the SSC process is at work, with the usual assumptions of one-zone models : the relativistic particles are assumed to be injected in a spherical homogeneous "blob" of radius R, moving at a relativistic velocity characterized by the Lorentz factor Γ and a corresponding Doppler factor δ. The blob is filled with a tangled magnetic field of constant strengh B. We will refer to all quantities expressed in source rest frame by a star and quantities in observer's frame are not labeled. All energies are expressed in reduced unit of $m_e c^2$. Throughout this paper, we express the Hubble parameter by $H_0 = 100\,h\,\mathrm{km\,s^{-1}\,Mpc^{-1}}$ and assuming h to be equal to $h = 0.65$.

2.1. The synchrotron and IC differential Luminosity

Inspection of the TeV blazars spectra shows that the IC spectra reaches their maximum luminosity at some peak energy ε_c, which is of the order of 10^6 for TeV photons. This energy corresponds to an energy $\varepsilon_c^* = \varepsilon_c \delta^{-1}$ in the blob frame. We will consider only the particles

emitting this typical energy via the IC process, which have a typical individual Lorentz factor (in the blob frame) γ_c, which must be greater than ε_c^*.
We then define another typical energy ε_s, that is emitted by synchrotron process by the same particles. It can be expressed in the blob frame as $\varepsilon_s^* = (B/B_0)\gamma_c^2$ where $B_0 = 3B_c/2$ and $B_c = 2\pi m_e^2 c^3/eh \approx 4.41 \times 10^{13}$G is the usual "QED critical magnetic field strength". One has then $\varepsilon_s = \delta(B/B_0)\gamma_c^2$. Synchrotron spectra of TeV blazars are typically peaking in the 1-100 keV range so that $\varepsilon_s \sim 10^{-2} - 10^{-1}$.
Synchrotron photons are up-scattered at high-energy via Inverse Compton process. It has been stressed by various authors that, giving the observed energies of IC and synchrotron photons, the collisions between the most energetic particles and the peak synchrotron photons take place in the Klein-Nishina regime, that is $\varepsilon_s^*\gamma_c \geqslant 1$. In this condition, the particle (electron or positron) gives all of his energy in a single interaction. It follows that $\gamma_c \sim \varepsilon_c^*$. This gives an estimate of the magnetic field strength,

$$B = B_0 \frac{\varepsilon_s^*}{(\varepsilon_c^*)^2} = \delta B_0 \frac{\varepsilon_s}{\varepsilon_c^2} \tag{1}$$

which is only valid in the Klein-Nishina scattering regime.

The differential synchrotron luminosity $L_{\varepsilon,s}$ per unit reduced energy emitted by a population of particles of energy γ at the energy ε_s with differential energy number of particles $\mathrm{d}N/\mathrm{d}\gamma$ reads

$$L_{\varepsilon,s}(\varepsilon_s) = \frac{\mathrm{d}L_s}{\mathrm{d}\varepsilon}(\varepsilon_s) = \delta^3 \frac{\mathrm{d}L_s^*}{\mathrm{d}\varepsilon^*}(\varepsilon_s^*) = \delta^3 \frac{\mathrm{d}L_s^*}{\mathrm{d}N}\frac{\mathrm{d}N}{\mathrm{d}\gamma}\frac{\mathrm{d}\gamma}{\mathrm{d}\varepsilon^*}. \tag{2}$$

The total power lost per particle of energy γ is given by the well-known relation $\mathrm{d}L_s^*/\mathrm{d}N = (4/3)c\sigma_{\mathrm{Th}}\gamma^2 W_B$, and we obtain,

$$L_{\varepsilon,s}(\varepsilon_s) = \delta \frac{4}{3} c\sigma_{\mathrm{Th}} W_B \frac{\varepsilon_c^3}{2\varepsilon_s}\frac{\mathrm{d}N}{\mathrm{d}\gamma} \tag{3}$$

where $W_B = B^2/8\pi$ is the usual magnetic energy density. Combining with equation (1), we can write :

$$L_{\varepsilon,s}(\varepsilon_s) = \delta^3 \frac{1}{6\pi} c\sigma_{\mathrm{Th}} B_0^2 \frac{\varepsilon_s}{\varepsilon_c}\frac{\mathrm{d}N}{\mathrm{d}\gamma}. \tag{4}$$

We can compute the differential IC luminosity $L_{\varepsilon,IC}(\varepsilon_c)$ in the same way using an expression-similar to Eq. 2, but replacing the magnetic energy density by the photon energy density. However we have to take into account that the Klein-Nishina cut-off reduces the effective energy density available for Inverse Compton scattering. We thus define a new characteristic energy, corresponding to the synchrotron photon energy at the limit between the Thomson and Klein-Nishina regime for particles with an energy γ_c. This energy is $\varepsilon_t^* = 1/\gamma_c$, i.e. in the observer's frame

$$\varepsilon_t = \delta^2/\varepsilon_c. \tag{5}$$

Photons of this energy will also be the main contributors for absorbing photons of energy ε_c to create electron/positron pairs.If we neglect the Klein-Nishina contribution above ε_t, the total power lost per particle of energy γ writes $\mathrm{d}L_c^*/\mathrm{d}N = (4/3)c\sigma_{\rm Th}\gamma^2 W_{\rm ph}^{\rm eff*}$, where

$$W_{\rm ph}^{\rm eff*} = \frac{L_s^{\rm eff*}}{4\pi R^2 c} = \frac{1}{4\pi R^2 c}\int_{\varepsilon^*_{\rm min}}^{\varepsilon_t^*} \mathrm{d}\varepsilon^* \frac{\mathrm{d}L_s}{\mathrm{d}\varepsilon^*}. \tag{6}$$

For a power-law spectrum $\nu F_\nu \propto \nu^\beta$ with $\beta > 0$, a simple calculation gives

$$W_{\rm ph}^{\rm eff*} \simeq \frac{1}{4\pi R^2 c}\frac{\delta^{-2}}{\beta\varepsilon_c} L_{\varepsilon,s}(\varepsilon_t).$$

The coefficient β can be replaced by another numerical coefficient close to 1 as long as the νF_ν spectrum is growing with energy. The differential IC luminosity reads then :

$$L_{\varepsilon,IC}(\varepsilon_c) = \delta^{-1}\beta^{-1}\frac{\sigma_{\rm Th}}{3\pi R^2}\,\varepsilon_c L_{\varepsilon,s}(\varepsilon_t)\frac{\mathrm{d}N}{\mathrm{d}\gamma}\,. \tag{7}$$

Comparing equation (4) and (7) we can now estimate the radius of source R as a function of observed luminosities and the unknown Doppler factor :

$$R = \delta^{-2}\frac{3eh}{2\pi m_e^2 c^{7/2}}\frac{\varepsilon_c}{\sqrt{\beta\varepsilon_s}}\left(\frac{L_{\varepsilon,s}(\varepsilon_t)L_{\varepsilon,s}(\varepsilon_s)}{L_{\varepsilon,IC}(\varepsilon_c)}\right)^{1/2}. \tag{8}$$

We will now use this radius estimate to compute the $\gamma-\gamma$ optical depth for the photons of energy ε_c.

2.2. The $\gamma-\gamma$ photon opacity

As we mention above, gamma-ray photons of energy ε_c^* are mainly absorbed by photons of energy $\varepsilon_c^{*-1} = \varepsilon_t^*$ creating pairs. So the same soft photons control both the amount of IC process and the absorption of IC photons. The absorption probability (or opacity) per unit path length of a photon of energy $\varepsilon_c^* \gg 1$ due to pair production in the case of a power-law SED is given approximately by

$$\ell_{\gamma\gamma}^{-1}(\varepsilon_c^*) = \frac{\mathrm{d}}{\mathrm{d}z}\tau_{\gamma\gamma}(\varepsilon^*) = \alpha_{\gamma\gamma}\sigma_{\rm Th}\varepsilon_t^* n(\varepsilon_t^*),$$

where $\ell_{\gamma\gamma}(\varepsilon^*)$ is the free mean path of the photon and $n(\varepsilon^*)$ the differential photon density per unit of reduced photon energy ε^*. In the framework of one-zone model, the typical interaction scale is of the order of the size of source R. It follows that the typical $\gamma-\gamma$ optical depth writes,

$$\tau_{\gamma\gamma}(\varepsilon^*) \approx \frac{R}{\ell_{\gamma\gamma}(\varepsilon^*)} = \alpha_{\gamma\gamma} R\sigma_{\rm Th}\varepsilon_t^* n(\varepsilon_t^*).$$

The function $\alpha_{\gamma\gamma}$ (Svensson 1987; Coppi & Blandford 1990) depends on the index β of the power-law of the spectral soft photon density expressed in $\nu F_\nu \propto \nu^\beta$ form. A commonly used value of $\alpha_{\gamma\gamma}(\beta)$ is 0.2 or 0.25. More precisely we have (Svensson 1987)

$$\alpha_{\gamma\gamma}(\beta) = 4^{1-\beta} 6 \times \frac{\Gamma^2(2-\beta)}{\Gamma(7-2\beta)} \times \frac{44-\beta(41-\beta(12-\beta))}{(4-\beta)(3-\beta)}. \tag{9}$$

The differential energy density number of particle is given as a function of the differential luminosity by

$$n(\varepsilon_t^*) = \frac{L^*_{\varepsilon,s}(\varepsilon_t^*)}{4\pi m_e c^3 R^2 \varepsilon_t^*}, \tag{10}$$

so we get finally the optical depth as a soft compactness at the energy ε_t:

$$\tau_{\gamma\gamma}(\varepsilon^*) = \alpha_{\gamma\gamma}(\beta) \frac{\sigma_{\rm Th} L^*_{\varepsilon,s}(\varepsilon_t^*)}{4\pi m_e c^3 R} = \delta^{-3}\ \alpha_{\gamma\gamma}(\beta) \frac{\sigma_{\rm Th} L_{\varepsilon,s}(\varepsilon_t)}{4\pi m_e c^3 R}. \tag{11}$$

Using our estimate on the source radius R equation (8), we obtain

$$\begin{aligned} \tau_{\gamma\gamma}(\varepsilon_c) &= \delta^{-1} \tilde{\alpha}_{\gamma\gamma}(\beta) \frac{\sigma_{\rm Th} m_e c^{1/2}}{6eh} \\ &\quad \times \frac{\sqrt{\varepsilon_s}}{\varepsilon_c} \left(\frac{L_{\varepsilon,s}(\varepsilon_t) L_{\varepsilon,IC}(\varepsilon_c)}{L_{\varepsilon,s}(\varepsilon_s)} \right)^{1/2}, \end{aligned} \tag{12}$$

where we introduce the modified function $\tilde{\alpha}_{\gamma\gamma}(\beta)$ as $\tilde{\alpha}_{\gamma\gamma}(\beta) = \alpha_{\gamma\gamma}\sqrt{\beta}$. Values of $\tilde{\alpha}_{\gamma\gamma}$ and $\alpha_{\gamma\gamma}$ for some β are tabulated in table 2.

2.3. Constraints on the local synchrotron spectral shape

Equation (2) shows that if we are able to measure the position in frequency and flux of both the synchrotron and the IC peak, then we can evaluate the optical depth to $\gamma-\gamma$ absorption at the IC peak as a function of the assumed Doppler factor value. This optical depth is controlled by the synchrotron luminosity at the frequency $\varepsilon_t = \delta^2/\varepsilon_c$. We can use this relation either by assuming some Doppler factor and evaluate the optical depth, or constrain the value of δ by limiting the value of $\tau_{\gamma\gamma}$. We can define $r_{\rm max}$, the Compton dominance parameter, as the ratio of IC luminosity's peak to the synchrotron one,

$$r_{\rm max} = \frac{[\nu_c F_c(\nu_c)]_{\rm max}}{[\nu_s F_s(\nu_s)]_{\rm max}} = \frac{\varepsilon_c L_{\varepsilon,IC}(\varepsilon_c)}{\varepsilon_s L_{\varepsilon,s}(\varepsilon_s)}. \tag{13}$$

We can rewrite equation (12) to express the luminosity at $\varepsilon_t = \delta^2/\varepsilon_c$ as a function of the optical depth and the $r_{\rm max}$ parameter. We finally obtain,

$$\varepsilon_t L_{\varepsilon,s}(\varepsilon_t) = \frac{\delta^4}{r_{\rm max}} \left[\frac{\tau_{\gamma\gamma}(\varepsilon_c^{\rm max})}{\tilde{\alpha}_{\gamma\gamma}(\beta)} \frac{6eh}{\sigma_{\rm Th} m_e c^{1/2}} \frac{\varepsilon_c^{\rm max}}{\varepsilon_s^{\rm max}} \right]^2. \tag{14}$$

Equations (5) and (14) can be considered as a system of two parametric equations of the curve giving $\varepsilon_t L_{\varepsilon,s}(\varepsilon_t)$ as a function of ε_t. Eliminating δ between the two previsously cited equation, one gets the following expression :

$$\varepsilon_t L_{\varepsilon,s}(\varepsilon_t) = \frac{\varepsilon_t^2 \varepsilon_c^2}{r_{\max}} \left[\frac{\tau_{\gamma\gamma}(\varepsilon_c^{\max})}{\tilde{\alpha}_{\gamma\gamma}(\beta)} \frac{6eh}{\sigma_{\rm Th} m_e c^{1/2}} \frac{\varepsilon_c^{\max}}{\varepsilon_s^{\max}} \right]^2 . \tag{15}$$

For nearby sources, the luminosity distance writes $d_\ell(z) \approx cz/H_0$ and previous expression can expressed in term on flux F instead luminosity L using the well known relation $F = L/4\pi d_\ell^2$,

$$\left(\nu_s \frac{{\rm d}F_s}{{\rm d}\nu_s} \right)_{\varepsilon_s \approx \delta^2/\varepsilon_c^{\max}} = 3.4 \times 10^{-36} \delta^4 \left[\frac{h}{z} \frac{\tau_{\gamma\gamma}(\varepsilon_c^{\max})}{\tilde{\alpha}_{\gamma\gamma}(\beta)} \frac{\nu_c^{\max}}{\nu_s^{\max}} \right]^2 r_{\max}^{-1} \tag{16}$$

For an observed SED and a given value of the opacity parameter $\tau_{\gamma\gamma}$, the only remaining unknown quantity in the previous equation is the beaming Doppler factor δ. Each value of δ gives a point in the $\log_{10}\nu - \log_{10}(\nu F_\nu)$ plane lying on straight line of slope 2, the level of the curve depending only on the value of $\tau_{\gamma\gamma}$. Intersection of the synchrotron spectrum with the straight line directly constrains the minimum value $\delta_{\min}(\tau_{\gamma\gamma})$ of the beaming Doppler factor required to avoid the $\gamma - \gamma$ absorption with an opacity value of $\tau_{\gamma\gamma}$ of the Inverse Compton bump (at the peak frequency).

2.4. Application to Markarian 501

We apply this calculation to the case of the Mrk 501 object during the period of the 1997 April 16 where the Beppo-SAX satellite (Pian et al. 1998) and the CAT imaging Atmospheric Čerenkov Telescope (Djannati-Ataï et al. 1999; Barrau et al. 1998) have recorded simultaneous data (see figure 2). All observational parameters we need in the equation (16) are reported Table 1 . We consider the two cases where we take into account, or not, the attenuation of the high energy component by cosmic diffuse infrared background (DIrB). This effect consists in the interaction of emitted gamma rays during their travel through the Universe with the photon field of the diffuse infrared background (DIrB) to create pairs (Gould & Schréder 1967a,b; Stecker, de Jager, & Salamon 1992; Vassiliev 2000). The tail of the high energy spectra is then de-reddened using the method described in Saugé & Henri (2004). This situation changes the position of Inverse Compton peak and the Compton dominance parameter $r_{\max}$. In this case, for $\tau_{\gamma\gamma} = 1$, we obtain both in the reddened and the de-reddened case $\delta_{\min}(1) \approx 50$ (see figure 3).

Given equation 16, the position of the line constraining δ depends on the value of $(\epsilon_c^{\max})^4/L_{\varepsilon,IC}$. It turns out that, also the IR un-folding of the spectrum changes both quantities, the previous ratio depends only slightly on the level of assumed absorption. The

value of $\delta_{\rm min}(1)$ are thus quite similar in the two cases because when we correct the Inverse Compton bump, position of the maximum moves both in luminosity and in frequency. This effect could be clearly seen on figure 3, where the difference between the two panels is hardly perceptible.

Note that in fact the level of the curve depends implicitly also on the value of modified power-law index of the spectrum β (see eq. [16]). In our case, we choose a value $\beta = 0.5$ directly measured on the SED.

2.5. Constraint from the variability timescale

Another constraint can be derived from the observation of short variability timescale. The classical argument is that a spherical static source cannot be variable on a timescale smaller than $R/\delta c$. So one gets an upper bound of radius of the source $R \leqslant R_{var,\rm min} = \delta c t_{var}$. Combining previous inequality to the equation (8) and expressing all the quantities in their fiducial units, we finally get a constraint similar to the one obtained in the previous section for the local synchrotron shape (see eq. [16]) :

$$\left(\nu_s \frac{{\rm d}F_s}{{\rm d}\nu_s}\right)_{\varepsilon_s \approx \delta^2/\varepsilon_c^{\rm max}} \leqslant 8.3 \times 10^{-26}\ \delta^8\ \left[\frac{h}{z}\frac{\nu_s^{\rm max}}{(\nu_c^{\rm max})^2} t_{var}\right]^2 r_{\rm max}^{-1}. \qquad (17)$$

Taking a characteristic variability timescale of roughly 15 min, we obtain the left solid thick line displayed on the figure 3. It appears that this constraint is less restrictive than the previous. In context of homogeneous modeling, it gives a minimum value for Doppler factor of 6–8 and 8–10 for the reddened and the de-reddened case respectively.

3. The case for low Lorentz factor

In this section we shortly review all the arguments and pieces of evidence in favour of moderate or low values of the bulk Lorentz factor.

3.1. Absence of superluminal motion at parsec scale

Observations at the VLBI scale (≈mas) show that blazars often display superluminal apparent velocities. This phenomenon predicted by Rees (1966) is expected for relativistic moving sources which is highly beamed and closely aligned with the observer's line of sight.

For a component moving along the jet axis at a reduced speed $\beta = v/c$ and making an angle θ from the line of sight, the apparent transverse velocity measured by the observer is :

$$\beta_{\rm app} = \frac{\beta \sin\theta}{1 - \beta\cos\theta} \leqslant \beta\Gamma. \tag{18}$$

If $\beta > \beta_{\rm crit} = \sqrt{2}/2$ and θ is such that $\sin 2\theta > (\Gamma^2 - 1)^{-1}$, the motion will appear to be superluminal *i.e.* $\beta_{\rm app} > 1$. Expressed in degrees the latter condition writes $\theta > \theta_{\rm crit} = 0.28\,(\Gamma/10)^{-2}$ deg.

As a matter of fact, VLBI/VLBA campaigns have not clearly succeeded in finding superluminal motion at the parsec scale for any TeV blazars (Edwards & Piner 2002; Piner & Edwards 2004). Observed radio components seem to be stationary or subluminal, requiring low or moderate values of the Lorentz factor ($\Gamma \approx 2 - 4$).
The absence of superluminal motion could be explained by a very close alignment of the jet with the line of sight. Indeed, following the previous expressions, if $\theta \leqslant 1/2\Gamma^2$ the apparent velocity is always smaller than c, and object appears to be subluminal despite the large value of Γ. But it this case, a simple statistical argument based on the density number of unbeamed counterparts rule out this possibility as we will see in the next section.

Moreover, derived value of the brightness temperature of the VLBI core is in the order of 10^{10-11} K and lie well below the usual Inverse Compton limit of $\approx 10^{11-12}$ K necessary to avoid the "Inverse Compton catastrophe", *i.e.* situation where ultra-relativistic particles suffer from dramatically Compton cooling in a very short time. Piner & Edwards (2004) have concluded that the jet should be only mildly relativistic at parsec scale. They propose that the TeV emitting inner jet is strongly decelerated before reaching the parsec scale. However we will see in the following that the existence of the highly relativistic motion is challenged by other observational facts concerning the statistics of beamed *vs.* unbeamed sources.

3.2. Number of beamed sources in the BL Lac/FR-I unification paradigm

As we said in the introduction, the blazar phenomenon arises from a close alignment of jet axis with the observer's line of sight. Following this scheme, one expects the existence of sources sharing the same physical properties (*i.e.* intrinsically the same objects), but viewed at larger angle. It has been proposed that Fanaroff-Riley radio galaxies can be the unbeamed parent population of blazars and particularly, FR-I galaxies can be the counterparts of Lacertids (Urry & Padovani 1995).

The unification hypothesis can be tested on samples of objects both by their luminosity ratio and by their spatial density. Doppler beaming effect enhances the intrinsic bolometric luminosity by a factor δ^4. The Doppler factor itself varies from $\delta_{\rm max} = 2\Gamma$ for a jet pointing exactly toward the observer, to $\delta_{\rm min} = 1/\Gamma$ for jets lying close to the sky plane. Although the exact definition of what is a beamed object can be somewhat subtle, one can estimate an order of magnitude of the number of such objects. It is easy to see that the solid angle for which the Doppler factor is larger than some given value δ_0 (where of course $\Gamma^{-1} < \delta_0 < 2\Gamma$ is

$$\Omega = 2\pi(1-\mu_0) \simeq \frac{2\pi}{\Gamma}\left(\frac{1}{\delta_0} - \frac{1}{2\Gamma}\right) \tag{19}$$

where we used $1/\beta \simeq 1 + 1/(2\Gamma^2)$, and hence the fraction of sources with a Doppler boosting larger than δ_0 is approximately

$$f(\delta > \delta_0) \simeq \frac{1}{\Gamma}\left(\frac{1}{\delta_0} - \frac{1}{2\Gamma}\right), \tag{20}$$

if we assume always two symmetrical jets.
So any "beaming criterion" imposing a Doppler factor larger than some sizable fraction of Γ will give a fraction of beamed sources of the order of Γ^{-2}. For one beamed source, one expects thus around Γ^2 unbeamed sources. It turns out that careful statistical studies do indeed confirm the association of BL Lac objects with FR-I galaxies, but they converge toward a much lower Lorentz factor than what is expected from the gamma-ray emission. For X-ray selected BL Lacs, which comprise all known TeV blazars, the inferred density ratio is 1:7, corresponding to a bulk Lorentz factor around 3.5 (Urry & Padovani 1995).

In the same way, we can examine the hypothesis that the lack of detection of superluminal motion would be due to a close alignment of the jet with the line of sight. As we note in the previous section, a beamed source with $\theta \leqslant 1/2\Gamma^2$ can not appear superluminal. The cone substained by this angle corresponds to the solid angle $\Omega \approx \pi/4\Gamma^4$. The ratio f' between the density of unbeamed sources and subluminal beamed sources one is thus given by

$$f' = \frac{n_{\rm FR-I}}{n_{\rm TeV,sub}} \approx 16\Gamma^4. \tag{21}$$

Observations show that 5 TeV blazars do not clearly display superluminal motions for $z_s \leqslant 0.047$ (Edwards & Piner 2002; Piner & Edwards 2004). Assuming $\delta = 2\Gamma = 50$, it corresponds roughly to a volume of 0.043 Gpc^3 and then to a density of subluminal TeV blazars of $n_{\rm TeV,sub} = 117$ Gpc^{-3}. Then, the density of expected unbeamed counterparts would be $n_{\rm FR-I} \approx 7.3 \times 10^8$ Gpc^{-3} which is absolutely unreasonable.

3.3. Luminosity ratio of beamed sources

in the BL Lac/FR-I unification paradigm

Another constraint can be derived from the luminosity ratio between the Lacertids sources and the FR-I ones. Supposing the same assumption as above (see previous section 3.2), *ie* Lacertids and FR-I are on average the same intrinsic objects but viewed at different angles, the bolometric luminosity contrast between the two parents population (Lacertids and FR-I radio galaxies) is given by,

$$\varpi = \frac{\mathcal{L}_{\rm Lac}}{\mathcal{L}_{\rm FRI}} = \left(\frac{\delta_{\rm Lac}}{\delta_{\rm FRI}}\right)^4. \tag{22}$$

In the case of Lacertids, relativistic beaming requires $0 \leqslant \theta \leqslant 1/\Gamma$ or equivalently $2\Gamma \geqslant \delta_{\rm Lac} \geqslant \Gamma$. On the other hand, we suppose that off-axis counterparts verify $\delta \approx 2/\Gamma$ (corresponding to an average angle value of $\theta \approx 60$ deg for $\Gamma > 1$). Then, equation (22) rewrites

$$\Gamma^8 \geqslant \varpi \geqslant \frac{\Gamma^8}{16}. \tag{23}$$

This estimate can of course be complicated by an intrinsic luminosity distribution. It may be also that we cannot detect the unbeamed sources due to limited sensitivity of the instrument. However some other indicators such as the extended radio lobes power or the galaxy luminosity itself are not highly beamed, and can serve as an unbiased criterion to select samples.

Capetti & Celotti (1999) studied a sample of 12 Lacertids and 5 FR-I sources with HST and compared the core luminosity ratio between objects sharing similar radiative properties. It clearly appears that the whole emission of the Lacertid cores is roughly 10^2–10^5 times brighter than the corresponding radio galaxy ones. Moreover Chiaberge et al. (2000) performed a similar work on a larger and more complete sample. They roughly obtained the same conclusions : the luminosity ratio between Lacertids and radio galaxy belongs to the interval $10^{2.5}$–$10^{5.5}$. Applying relation (23), we obtain typical values of $\Gamma \approx 2$–5 for the bulk Lorentz factor. They also compare the broad band spectra of both classes of objects and they found that the spectra could be deduced by a simple Doppler boosting, but once again with modest values of the Doppler factor.

3.4. Detection of TeV unbeamed source – the case of M87

The nearby giant elliptical radio galaxy M87 (NGC4486, $z_s \approx 0.00436$) is the first (and for the time being unique) detected unbeamed radio-loud source at the TeV energy range.

First detection was reported by the HEGRA collaboration with an integral flux above 250 GeV at about 3.3% of the flux of the Crab Nebula (with a significance of $4.7\,\sigma$) during an high state (Aharonian et al. 2003; Beilicke et al. 2004). Such TeV events are confirmed by recent measurements of *High Energy Stereoscopic System* (HESS) (Beilicke et al. 2005). The powerful radio jet of M87 has been well studied in various wavelengthes from radio to X-rays, showing that the jet axis makes an angle between 30 and 40 deg with the line of sight. This angle is clearly large enough to ensure that the emission is unbeamed. Previous works based on the study of the proper motion of the VLBI knots (Biretta et al. 1995) or on the detailed analysis of HST and VLA observations (Lobanov et al. 2003) converge toward value for Γ of 3–5 at the kiloparsec scale. The jet differential flux of a source expressed in the observer's frame can be written as function of the intrinsic differential luminosity as

$$\mathcal{F}_\nu(\nu;\theta,z) \approx (1+z)\delta^3\ \frac{\mathcal{L}^*_\nu(\nu^*)}{4\pi d_\ell^2}, \tag{24}$$

with $\nu = \nu^*\delta/(1+z)$ and where $d_\ell(z) \approx zc/H_0$ is the usual luminosity distance. We now consider two different versions of the same intrinsic object, a beamed one corresponding to a blazar and an unbeamed one corresponding to a radio galaxy. In this case, the ratio $\mathcal{R}$ of the observed photon fluxes above some threshold frequency $\nu^{\rm thr}$ writes,

$$\begin{aligned}\mathcal{R} = \frac{\int_{\nu^{\rm thr}} {\rm d}\nu\,[\mathcal{F}^u_\nu(\nu)/h\nu]}{\int_{\nu^{\rm thr}} {\rm d}\nu\,[\mathcal{F}^b_\nu(\nu)/h\nu]} &= \left(\frac{z_b}{z_u}\right)^2 \left(\frac{1+z_b}{1+z_u}\right)^{\alpha-2} \left(\frac{\delta_u}{\delta_b}\right)^{2+\alpha}, \\ &= k(z_b,z_u;\alpha)\left(\frac{\delta_u}{\delta_b}\right)^{2+\alpha},\end{aligned} \tag{25}$$

where the index $_u$ (resp. $_b$) refers to the observed unbeamed (resp. beamed) quantities, and where we suppose that the high energy spectrum can be expressed as a simple power-law with a photon index α.

For beamed sources, the Doppler factor can be written as $\delta_b \approx 2\Gamma$ while for the unbeamed case one has $\delta_u = 1/\Gamma(1-\beta\cos\theta) < \Gamma$ with $\beta \approx 1 - 1/2\Gamma^2$. Finally we can express the bulk Lorentz factor as a function of θ and the observational parameters only

$$\Gamma(\theta) = \left\{\frac{\left[k(z_b,z_u;\alpha)\mathcal{R}^{-1}\right]^{1/(2+\alpha)} - \cos\theta}{2(1-\cos\theta)}\right\}^{1/2}. \tag{26}$$

A raw approximation of the previous expression is

$$\Gamma(\theta) \approx \frac{1}{\theta}\left[\frac{k(z_b,z_u;\alpha)}{\mathcal{R}}\right]^{1/2(2+\alpha)}, \tag{27}$$

showing the $\sim 1/\theta$ functional dependence of Γ and its slow power-law variation with $\mathcal{R}$ (or k). For instance, for a typical value of $\alpha = 2.5$, a factor ten on $\mathcal{R}$ implies only a factor ($10^{1/9} \approx 1.29$) on Γ.

In 1997 April flaring period, the TeV blazar Mrk 501 ($z_s \approx 0.034$) became roughly 8 times as bright as the Crab Nebula as reported by the French collaboration CAT (Djannati-Ataï et al. 1999). Assuming M87 is an unbeamed counterpart of Mrk 501 with an angle $30\,\mathrm{deg} \leqslant \theta_{\mathrm{M87}} \leqslant 40\,\mathrm{deg}$ we obtain $4 \leqslant \Gamma \leqslant 5.3$. Again we find that the luminosity ratio is compatible with modest values of the Lorentz factor. Due to the increasing sensitivity of the present and the next generation of the Imaging Atmospheric Čerenkov Telescope Arrays, the detections of more and more TeV radio galaxies should help us to constrain the dynamics of the emitting plasma at the subparsec scale in a more reliable statistical way.

3.5. Summary

All the above considerations show that observational data are compatible with the beaming model only if the bulk Lorentz factor for the X-ray and TeV emitting part of the object is relatively low, between 3 and 5. This value reproduces correctly the luminosity ratio *and* the statistical number of sources (which are a priori independant factors). Conversely, a value of $\Gamma = 12.5$ which is the minimum typical value derived from the one-zone modeling approach, would lead to a luminosity contrast of $\varpi \approx 10^{7.6}$–10^{9}. This latter estimation is clearly not compatible with the previous observations, ascertaining the "*Bulk Lorentz factor crisis of TeV blazars*". In the following, we will examine some suggestions made by various authors to solve the crisis.

4. How to solve the crisis

4.1. Two pattern model

Chiaberge et al. (2000) and Trussoni et al. (2003) argue that a jet velocity structure can solve the problem of the BL Lac/FR-I unification scheme. They consider a (med-)relativistic external layer and a fast internal spine which dominates the emission in the case of a favorable alignment along the observer's line of sight, *i.e.* in the blazar case. Although similar in appearance to the two-flow model of Pelletier (1985) (*see below for details*), it differs by the fact that both flows are relativistic, one with a "low" Lorentz factor (around 3) and one with a high Lorentz factor (at least 10). In the following, we consider the same approach considering a two-components modeling of the velocity structure, where a fast inner structure is supposed to be surrounded by a slow one. Each of these components is respectively characterized by a bulk Lorentz factor Γ_{f} and Γ_{s}. As we saw, the radiative emission of the moving source with a bulk Lorentz factor Γ is beamed in a cone sustained

by a solid angle $\delta\Omega = \pi/\Gamma^2$ along the motion. Therefore the emitted radiation appears to be Doppler boosted when the jet lies into $\delta\Omega$ around the observer's line of sight. In this case, the luminosity contrast between the two parents population (Lacertids and FR-I radio galaxies) writes,

$$\Gamma_{\rm s}^8 \leqslant \varpi \leqslant (\Gamma_{\rm s}\Gamma_{\rm f})^4, \tag{28}$$

where right and left bound correspond to the case where fast velocity component respectively dominates or not the emission. Unification models are sensitive to the slow component only, so ($\Gamma_{\rm s} = 3 - 5$) (Hardcastle et al. 2003; Trussoni et al. 2003; Chiaberge et al. 2000; Urry & Padovani 1991). Therefore, assuming $\Gamma_{\rm s} \approx 4$ we obtain $10^{4.81} \leqslant \varpi \leqslant 10^8$ if $\Gamma_{\rm f} = 25$ and $10^{4.81} \leqslant \varpi \leqslant 10^{6.4}$ if $\Gamma_{\rm f} = 10$.
The results give a possible solution to the luminosity ratio problem, being more compatible with observations. But in the next section we will examine the consequences of such a velocity structure on the detection probability of TeV emitters among BL Lac objects.

4.1.1. Statistics of detected sources

Suppose a population Σ of sources randomly oriented per unit volume n_0. Then the density number of sources oriented with an angle $\theta = \cos^{-1}\mu$ according to the observer's line of sight is $\mathrm{d}n/\mathrm{d}\mu = n_0/2$. We define BL Lac sources as those seen into the $\delta\Omega_{\rm s} = \pi/\Gamma_{\rm s}^2$ cone and therefore the TeV emitters as the part of Lacertids lying into the $\delta\Omega_{\rm f} = \pi/\Gamma_{\rm f}^2$. Therefore the probability of detecting a BL Lac object in Σ writes

$$\mathcal{P}_{\rm Lac} = \mathcal{P}(\mu \leqslant \mu_0) = \frac{1}{n_0}\int_1^{\mu_0} \mathrm{d}\mu\, \frac{\mathrm{d}n}{\mathrm{d}\mu} = \frac{1}{4\Gamma_{\rm s}^2}, \tag{29}$$

where $\mu_0 = 1 - 1/2\Gamma_{\rm s}$. The probability that a BL Lac object $\omega \in \Sigma$ is also a TeV emitter source (*i.e.* a source which the emission is dominated by the fast inner structure) is given by the conditional probability,

$$\mathcal{P}_{\rm TeV/Lac} = \mathcal{P}(\omega \in \mathrm{TeV} | \omega \in \mathrm{Lac}) = \left(\frac{\Gamma_{\rm s}}{\Gamma_{\rm f}}\right)^2. \tag{30}$$

The probability of detecting n TeV emitters among a population of N Lacertids is given by the usual binomial probability law,

$$\mathcal{P}(n/N) = \frac{N!}{n!(N-n)!}\,\mathcal{P}_{\rm TeV/Lac}^n (1 - \mathcal{P}_{\rm TeV/Lac})^{N-n}. \tag{31}$$

and implicitly depends on the value of the ratio $\Gamma_{\rm s}/\Gamma_{\rm f}$. It is more convenient to express the probability of detection of at least n TeV emitters among the same sample of N Lacertids

which writes,

$$\mathcal{P}(N \geqslant n_0 \geqslant n) = \sum_{k=n}^{k=N} \mathcal{P}(k/N). \tag{32}$$

4.1.2. Applications

For a given value of (n, N), requiring that $\mathcal{P}(N \geqslant n_0 \geqslant n)$ is larger than an a priori probability $\mathcal{P}_0$ constrains the space parameters $(\Gamma_\mathrm{s}, \Gamma_\mathrm{f})$. The latter inequality leads to eliminate parameter's region lying above a straight line which corresponds equivalently to a constant value of $\mathcal{P}_0$ or of the ratio $\Gamma_\mathrm{s}/\Gamma_\mathrm{f}$ (see eq. [32], [31] and [30]). Further restriction come from the $\gamma-$rays transparency argument and FR-I/Lacertids unification models as developed above.

1. Firstly, the $\gamma-$rays transparency argument developed in the first part of this work directly constrains the value of the fast component as it requires a minimum value of the Doppler factor δ_min, and therefore $\Gamma_\mathrm{f} \geqslant \delta_\mathrm{min}/2$. We have shown that $\delta_\mathrm{min} \approx 50$ exclude all part of the $(\Gamma_\mathrm{s}, \Gamma_\mathrm{f})$ lying above $\Gamma_\mathrm{f} = 25$.

2. Secondly, basic statistics argument based on the number FR-I radio galaxies regarding the Lacertid one and the comparison of luminosity distribution of the previous populations constrain the value of the slow component to reasonable values less than $\Gamma_\mathrm{s} \approx 7$ (Urry & Padovani 1995; Chiaberge et al. 2000).

We test this result on the catalog of BL Lac objects from Padovani & Giommi (1995). At $z_s \leqslant 0.13$ they report 29 Lacertids with known redshift. Setting $(n = 7, N = 29)$, $\mathcal{P}_0 = 1\%$ and recalling that $\Gamma_\mathrm{s,max} = 7$ and $\Gamma_\mathrm{f,min} = 25$, the intersection of all listed previous constraints reduces to null region (see figure 5). Even with the hypothesis of a structured flow, a large value of the Lorentz factor recquired by one-zone homogeneous models is clearly untenable (excluded with a confidence level of 99%).

We demonstrate that even if the two-components velocity structure can give a satisfactory answer to the luminosity problem of the Lacertids even with large value of Doppler factor required by high energy emission models, it fails to explain the detection statistics of the TeV emitters among the BL Lac object population supposed to be off-axis FR-I sources.

5. Discussion

5.1. Inhomogeneous models

Altogether, the previous considerations lead to a serious paradox, where a high Lorentz factor larger than 20 seems mandatory to avoid strong $\gamma - \gamma$ absorption, whereas all other facts tend to favour modest values around 3. The only way to solve the discrepancy seems to give up the implicit assumption of all one zone model, i.e. the fact that all photons are produced co-spatially and simultaneously in some characteristic region of size R. Alternative to one-zone models have already been discussed in the literature. For instance, in the "blob-in-jet" model (Katarzyński et al. 2001, 2003), low energy photons are produced in a continuous jet and only the high energy ones are produced in a spherical blob. This allow to fit the overall spectrum with a smaller Doppler factor of around 15. Another possibility is to take explicitly the variability and use a time-dependant model to reproduce the data. Again, the constraints arising from $\gamma - \gamma$ opacity can be somewhat released because soft photons are emitted at a later stage than high energy ones. As has been remarked by Ghisellini et al. (1985), time-dependant model will produce effects comparable to inhomogeneous ones. If the evolving source is moving at relativistic velocity, and that many flares are contributing to the emission, the overall system will be in fact an stratified jet composed with many "one-zone" regions in a different evolutionary stage. However, none of these models do use bulk Lorentz factors as low as 3.

We are led thus to consider models where photons are distributed along a jet in a continuous structure, instead of filling a spherical source. In this case, the luminosity is proportional to the photon density times the lateral surface of the jet, which is $2\pi R_j h_j = 2\pi A R_j^2$, where R_j and h_j are the typical jet radius and length at the emission region, and $A = h_j/R_j$ is an aspect ratio of the source. For a self similar jet for which all quantities (radius, magnetic field, particle density etc...) are described by power law as a function of the distance z, one expects $h_j \sim z_j$, where z_j is the distance of the emitting region from the center. It follows that $A \sim z_j/R_j \sim \theta_j^{-1}$, where θ_j is the typical opening angle of the jet. One can see that for a given synchrotron luminosity and photon density (implying the same IC luminosity), one must conserve the quantity AR_j^2, so the typical radius of the jet, and hence the $\gamma - \gamma$ optical depth will be reduced by a factor $A^{1/2}$ with respect to a spherical source. This simple geometrical modification helps thus to increase luminosity without increasing optical depth. Furthermore, the particle distribution needs not to be the same all along the jet. Rather one expects a gradual cooling of the particles, the overall spectrum being the envelope of all slices of the jet. The local photon spectrum can thus be different from the observed one, and particularly the local soft photon density can be much lower, helping again

to reduce the $\gamma - \gamma$ optical depth. As we shall see, all these factors can offer a clue to the Bulk Lorentz factor crisis, but imply strong constraints on the physical picture of relativistic jets.

5.2. Theoretical implications

5.2.1. Local photon density

Considering the above constraints, we will take the opposite attitude, considering that the value of the bulk Lorentz factor is constrained by the unification models and the detection of unbeamed sources to be around 3. The typical high energy emission zone as defined above is equivalent to the superposition of A spherical sources with individual luminosities $L_\nu/A \sim \theta_j L_\nu$. Therefore, all previous equations in section 2 are still valid provided we replace the observed luminosity L_ν by $\theta_j L_\nu$. Using equation (12), we conclude that all opacity constraints remain unchanged if we replace the optical depth $\tau_{\gamma\gamma}$ by $\theta_j^{-1/2}\tau_{\gamma\gamma}$, which is of course in accordance with the estimate made in the previous paragraph. So we can use the figure 3 with slightly different values of $\tau_{\gamma\gamma}$. The typical angle θ_j must be of the order of $10^{-2} - 10^{-1}$, so the optical depth will be reduced by a factor between 3 and 10. In the following, we will still use the same line $\theta_j^{-1/2}\tau_{\gamma\gamma} \approx 1$ to constrain the optical depth, meaning that $\tau_{\gamma\gamma} \leqslant 0.1$ to 0.3.

5.2.2. Local photon spectrum

We can thus put an upper limit on the soft photon luminosity corresponding to this value and a Doppler factor of 3, which constrains the soft photon luminosity at an energy $\varepsilon_t = \delta^2/\varepsilon_c \sim 10$ eV. As the spectrum is by definition approximately the same in all the characteristic emission region, we can thus estimate the local photon spectrum by interpolating between the peak synchrotron luminosity and the above upper limit. Inspection of figure 3 shows that the spectral index between 10 eV and 100 keV is very close to 1/3, which is characteristic of a quasi monoenergetic distribution; an example of such distribution is provided by the quasi-maxwellian or "pileup" distribution (Henri & Pelletier 1991; Schlickeiser 1985; Saugé & Henri 2004), which is a natural outcome of some acceleration processes like second order Fermi acceleration or magnetic reconnexion. This distribution is not the usual power law often claimed to exist in AGN, and which is naturally produced in MHD shocks. Rather than localized shocks, the assumption of low Lorentz factor leads to a picture of a

continuous jet filled by relativistic particles, continuously reheated by a diffuse acceleration mechanism.

5.2.3. Pair production

The local synchrotron spectrum can not be harder than the monoenergetic one; so figure 3 proves that this implies a lower limit to the quantity $\theta_j^{-1/2}\tau_{\gamma\gamma} \gtrsim 1$. Thus the limit on $\gamma - \gamma$ optical depth can not be very low, unless we have an extremely well collimated jet that is not supported by the general FR-I morphology. Modest collimation factors imply that $\tau_{\gamma\gamma} \gtrsim 0.1$. This supports the formation of an electron-positron pair plasma in the acceleration site. If the acceleration is not localized, which is suggested by the picture of a continuous jet filled by a pile-up distribution, the pairs created by $\gamma - \gamma$ interaction can not avoid being reaccelerated and will trigger a pair cascade (Henri & Pelletier 1991). These constraints are thus suggestive of a inner continuous pair dominated, jet-like emission zone, maintained at a relativistic temperature.

5.3. Compatibility with the two-flow model

All the previous considerations find a natural explanation in the context of the two-flow model, which was proposed to account for the formation of relativistic jets in AGN : in this model, extragalactic jets are in fact the results of a double structure: a first jet, not highly but only mildly relativistic ($v \approx 0.5c$), is emitted by a MHD mechanism by a large scale magnetic field anchored in an accretion disk (Blandford & Payne 1982; Ferreira & Pelletier 1993a,b, 1995) ; this powerful, but weekly dissipative jet, can sustain a MHD turbulence able to accelerate non thermal particles. These particles will produce synchrotron and gamma-rays photons, and if the optical depth becomes large enough, these photons will trigger an intense pair cascade leading to a dense pair plasma in the empty "throat" of the jet. We have shown in previous works that this pair plasma will be spontaneously accelerated to relativistic velocities even if the surrounding jet is not highly relativistic by itself, by the so called "Compton Rocket effect", which is a recoil effect associated with anisotropic IC process originally introduced by Odell (1981). The Compton Rocket effect has been shown to be inefficient to accelerate an *isolated* relativistic plasma because the cooling time is always shorter than the bulk acceleration time (Phinney 1982). In the two-flow model however, the heating by the surrounding jets compensates for the cooling and the pair plasma remains relativistic over large distances (Marcowith, Henri, & Pelletier 1995).

Detailed calculations of the Compton Rocket effect in this configuration (Renaud & Henri 1998) show that the pair plasma accelerates gradually in the vicinity of an accretion disk, being maintained to a quasi equilibrium Lorentz factor $\Gamma_{\rm beq} \approx (z/r_i)^{1/4}$, where r_i is the inner radius of the accretion disk (3 gravitational radii for a Schwarschild black hole). The equilibrium Lorentz factor is defined by the fact that the photon field of the accretion disk, *seen in the comoving frame*, appears to be nearly isotropic due to relativistic aberration. It grows slowly with the distance,because the field becomes more and more anisotropic. The acceleration continues until the photon density becomes to low to efficiently accelerate the plasma. Then the plasma decouples from the ambient radiation field and ends up with an asymptotic balistic motion at constant $\Gamma_{\rm b} \rightarrow \Gamma_{\rm b\infty}$, which depends on the disk luminosity and the particle energy distribution. For a relativistic energy distribution function $n(\gamma) \propto \gamma^2 \exp(-\gamma/\bar{\gamma})$, the asymptotic bulk Lorentz factor is approximately $\Gamma_{\rm b\infty} \approx (\ell_s \bar{\gamma})^{1/7}$, where $\ell_s = L_s \sigma_{\rm Th}/4\pi m_e c^3 r_i$ is the soft photon disk compactness and $\bar{\gamma}$ is the characteristic energy of the pileup depending on the details of the acceleration/cooling processes (Renaud & Henri 1998).

The first interesting feature in this model is that it predicts naturally a gradual acceleration from the core. The value of $\Gamma_{\rm b} \approx 3$ is naturally obtained at $\approx 100\ r_g$, which is a typical distance where gamma-ray emission seems to occur, based on variability arguments. Thus low Lorentz factor are not surprising in this model, but are explained naturally. As a matter of fact, very high values of 20 near the core would be difficult to explain in this frame!

The second one is that the asymptotic bulk Lorentz factor is controlled by the density of the photon field emitted by the accretion disk. For BL Lac objects and FR-I galaxies, the disk luminosity is known to be much lower than luminous FSRQ and FR-II galaxies, by a factor around 10^{-3}. One would expect thus a lower asymptotic Lorentz factor for BL Lac object in average, which would help to understand the absence of superluminal motion in TeV blazars. As a matter of fact, numerical estimates show that the expected asymptotic Lorentz factors are between 10 and 20 for near-Eddington accreting supermassive black holes, whereas they are rather between 5 and 10 for low luminosity AGN. We note that bulk Lorentz factors around 5 are indeed observed in M87, which would mean that the decoupling occurs at some thousands Schwarzschild radii from the core. Unification models are compatible with slowly accelerating jets, the inner (X-ray emitting) jets having bulk Lorentz factors around 3 and the outer radio jet having a larger Lorentz factor around 7 (Urry & Padovani (1995)). Again this is perfectly compatible with the predictions of the two-flow model, with an inner jet emitting X-ray and TeV radiation with a modest bulk Lorentz factor, and an outer jet responsible for radio emission with a higher one. Also we note that there is no

need for deceleration to explain FR I mildly relativistic jets : even if the large scale jet has only a moderately relativistic velocity $v \approx 0.5c$, this can be attributed to the "slow" MHD component surrounding the relativistic beam, the latter being dissipated at kpc scale.

An inhomogeneous model offers also a convenient explanation for the lack of obvious correlation between X-rays and gamma-rays variability. If the magnetic field is varying along the jet, the photons with a given energy could be produced by electrons with different energies and locations. If several flares contributes to the observed spectrum — which is necessary to account for the global spectral shape in case of a monoenergetic distribution — a complicated variability pattern could emerge. This is much less easy to understand in the homogeneous steady state models. Thus we think that inhomogeneous models, although more complicated to compute, seem to be unavoidable to explain the spectral and temporal features of TeV blazars' emission.

6. Conclusion

We have investigated in detail the so-called "Bulk Lorentz factor" crisis of TeV blazars, which seem to imply an incompatibility between a high Lorentz factor required to insure gamma-ray transparency, and a low Lorentz factor deduced from statistical arguments and luminosity contrast, including the detection of the non-blazar TeV source M87. We show that the transparency argument is common to all one-zone models, and that the only way of solving the paradox is to consider inhomogeneous jet models, where all photons are not produced cospatially. The spectrum is then the spatial convolution of different jet slices, and the opacity problem can be avoided by invoking geometrical arguments and harder local photon spectrum. We show however that for modest values of geometrical beaming of the jet, which seem natural considering the morphology of FR-I galaxies, the optical depth for $\gamma - \gamma$ absorption can not be very low, even for a local quasi-monoenergetic particle distribution. This has profound implications on the physics of the jet : the acceleration mechanism must be distributed all along the jet, and is more probably insured by second order Fermi mechanism or reconnexion sites than by localized shocks . A moderately high value of $\gamma - \gamma$ optical depth implies a fair production rate of electron-positron pairs, which are likely to be reaccelerated by the acceleration process to trigger a pair cascade. All this features are natural consequences of the two-flow model, which attributes the relativistic phenomena (high energy emission and superluminal motion) to the formation of such a pair plasma inside a powerful, but mildly relativistic jet insuring the confinement and the heating of the relativistic beam. The bulk Lorentz factor is also well in accordance with a continuous acceleration along the jet by the Compton Rocket effect, which predicts naturally $\Gamma_{\rm b} \approx 3$

at a hundred Schwarzschild radii from the core. We conclude that all observational facts are more in accordance with light, moderately relativistic leptonic beams than with highly relativistic baryonic jets.

Remarks of an anonymous referee helped to improve significantly the final version of this paper. L.S. would like to thank all members of the IPNL team of the SNFactory collaboration. Part of the simulations reported here has been performed at the "*Centre de Calcul Intensif de l'Observatoire de Grenoble.*".

REFERENCES

Aharonian, F., et al. 2005, A&A, 430,865A

Aharonian, F., et al. 2005, A&A, 436, L17

Aharonian, F., et al. 2004, A&A, 421, 529

Aharonian, F., et al. 2003, A&A, 403, L1

Barrau A. et al. 1998, Nucl. Instrum. Methods Phys. Res A, 416, 278

Beilicke, M., Götting, N., & Tluczykont, M. 2004, New Astronomy Review, 48, 407

Beilicke, M., et al. 2005, conference proceedings paper of the XXII Texas Symposium on Relativistic Astrophysics, Stanford University (California), preprint (astro-ph/0504395)

Biretta, J. A., Zhou, F., & Owen, F. N. 1995, ApJ, 447, 582

Blandford, R. D. & Payne, D. G. 1982, MNRAS, 199, 883

Blandford, R. D. & Znajek, R. L. 1977, MNRAS, 179, 433

Capetti, A., & Celotti, A. 1999, MNRAS, 304, 434

Catanese, M., et al. 1998, ApJ, 501, 616

Chiaberge, M., Celotti, A., Capetti, A., & Ghisellini, G. 2000, A&A, 358, 104

Coppi, P. S. & Blandford, R. D. 1990, MNRAS, 245, 453

Djannati-Ataï, A. et al. 1999, A&A, 350, 17

Edwards, P. G. & Piner, B. G. 2002, ApJ, 579, L67

Ferreira, J., & Pelletier, G. 1993a, A&A, 276, 625

Ferreira, J., & Pelletier, G. 1993b, A&A, 276, 637

Ferreira, J., & Pelletier, G. 1995, A&A, 295, 807

Gaidos, J. A., et al. 1996, Nature, 383, 319

Georganopoulos, M. & Kazanas, D. 2003, ApJ, 594, L27

Padovani, P. & Giommi, P. 1995, MNRAS, 277, 1477

Ghisellini, G., Maraschi, L., & Treves, A. 1985, A&A, 146, 204

Gould, R. J. & Schréder, G. P. 1967a, Physical Review , 155, 1404

Gould, R. J. & Schréder, G. P. 1967b, Physical Review , 155, 1408

Hardcastle, M. J., Worrall, D. M., Birkinshaw, M., & Canosa, C. M. 2003, MNRAS, 338, 176

Henri P., Pelletier G. 1991, ApJ, 383, L7

Katarzyński, K., Sol, H., & Kus, A. 2001, A&A, 367, 809

Katarzyński, K., Sol, H., & Kus, A. 2003, A&A, 410, 101

Konopelko, A. K., Mastichiadis, A., Kirk, J. G., de Jager, O. C., & Stecker, F. W. 2003, preprint (astro-ph/0302049)

Lobanov, A., Hardee, P., & Eilek, J. 2003, New Astronomy Review, 47, 629

Marcowith, A., Henri, G., & Pelletier, G. 1995, MNRAS, 277, 681

Marscher, A. P. 1983, ApJ, 264, 296

Odell, S. L. 1981, ApJ, 243, L147

Pelletier G. 1985, in proceedings "Plasma turbulence and Astrophysical Objects", SFP

Pelletier G., Sol H. 1992, MNRAS, 254, 635

Phinney, E. S. 1982, MNRAS, 198, 1109

Pian, E. et al. 1998,ApJ, 492, L17

Piner, B. G. & Edwards, P. G. 2004, ApJ, 600, 115

Protheroe, R. J. & Stanev, T. 1999, Astroparticle Physics, 10, 185

Punch, M., et al. 1992, Nature, 358, 477

Quinn, J., et al. 1996, ApJ, 456, L83

Rees, M. J., Nature, 211, 468

Rees, M. J., & Simon, M. 1968, ApJ, 152, L145

Renaud, N. & Henri, G. 1998, MNRAS, 300, 1047

Rybicki, G. B. & Lightman, A. P. 1979, Radiative Processes in Astrophysics (New York: Wiley-Interscience)

Saugé, L., & Henri, G. 2004, ApJ, 616, 136

Schlickeiser, R. 1985,A&A, 143, 431

Stecker, F. W., de Jager, O. C., & Salamon, M. H. 1992, ApJ, 390, L49

Svensson, R. 1987, MNRAS, 227, 403

MacDonald, D. & Thorne, K. S. 1982, MNRAS, 198, 345

Tavecchio, F., Maraschi, L., & Ghisellini, G. 1998, ApJ, 509, 608

Trussoni, E. el al. 2003, A&A, 403, 889

Urry, C. M. & Padovani, P. 1991, ApJ, 371, 60

Urry, C. M. & Padovani, P. 1995, PASP, 107, 803

Vassiliev, V. V. 2000, Astroparticle Physics, 12, 217

Zensus, J. A. 1997, ARA&A, 35, 607

Table 1. Mkn 501 1997 April-16 observationnals parameters

DiRB status	Synchrotron bump		Inverse Compton bump		
	$\log_{10}\nu_s^{\max}$	$\log_{10}\left(\nu_s\frac{\mathrm{d}F_s}{\mathrm{d}\nu_s}\right)_{\max}$	$\log_{10}\nu_c^{\max}$	$\log_{10}\left(\nu_c\frac{\mathrm{d}F_c}{\mathrm{d}\nu_c}\right)_{\max}$	$r_{\max}$
reddened	19.3 ± 0.1	-9.11 ± 0.04	26.4 ± 0.1	-9.46 ± 0.04	0.4467
de-reddened			26.6 ± 0.1	-9.04 ± 0.04	1.175

Table 2. Values of function $\alpha_{\gamma\gamma}(\beta)$ and the modified function modified function $\tilde{\alpha}_{\gamma\gamma}(\beta)$ as function as the spectral index β in νF_ν.

β	0	$\frac{1}{2}$	1	$\frac{4}{3}$
$\alpha_{\gamma\gamma}(\beta)$	0.122	0.236	0.583	1.397
$\tilde{\alpha}_{\gamma\gamma}(\beta)$	–	0.043	0.583	1.613

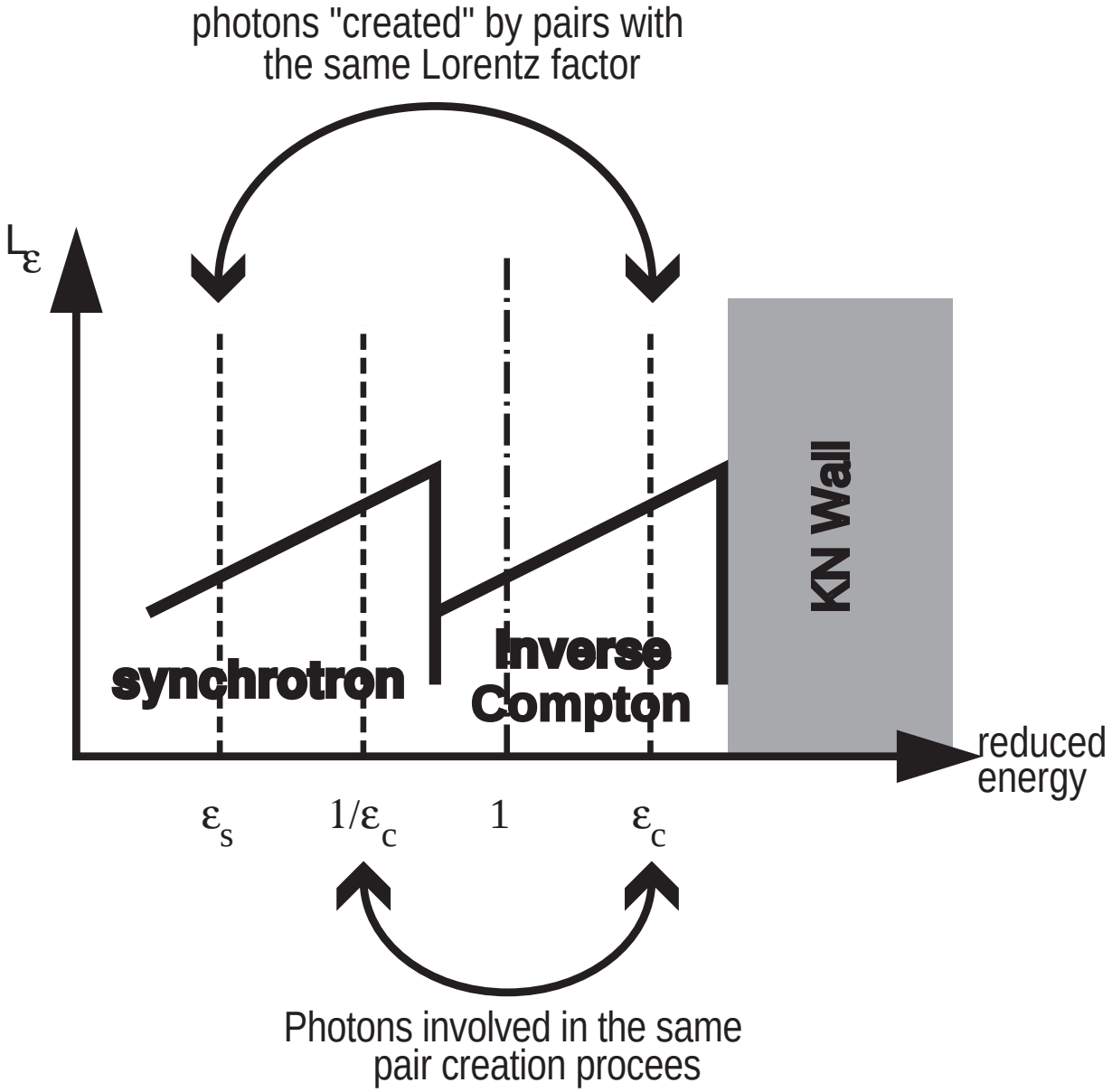

Fig. 1.— Working figure – High energy photons with reduced energy ε_c^* interact preferentialy with soft photons of energy $1/\varepsilon_c^*$ to create new pairs. In the Klein-Nishina scatering regime, an ultrarelativistic particle of reduced energy $\gamma = \varepsilon_c^*$ "create" a high energy photon with the same energy ε_c^*, and in the same time, other pairs with the same energy can create soft photons by synchroton process of energy $\varepsilon_s^* = (3eh/4\pi m_e^2 c^3)\, B\gamma^2 = (B/B_0)\, \gamma^2$.

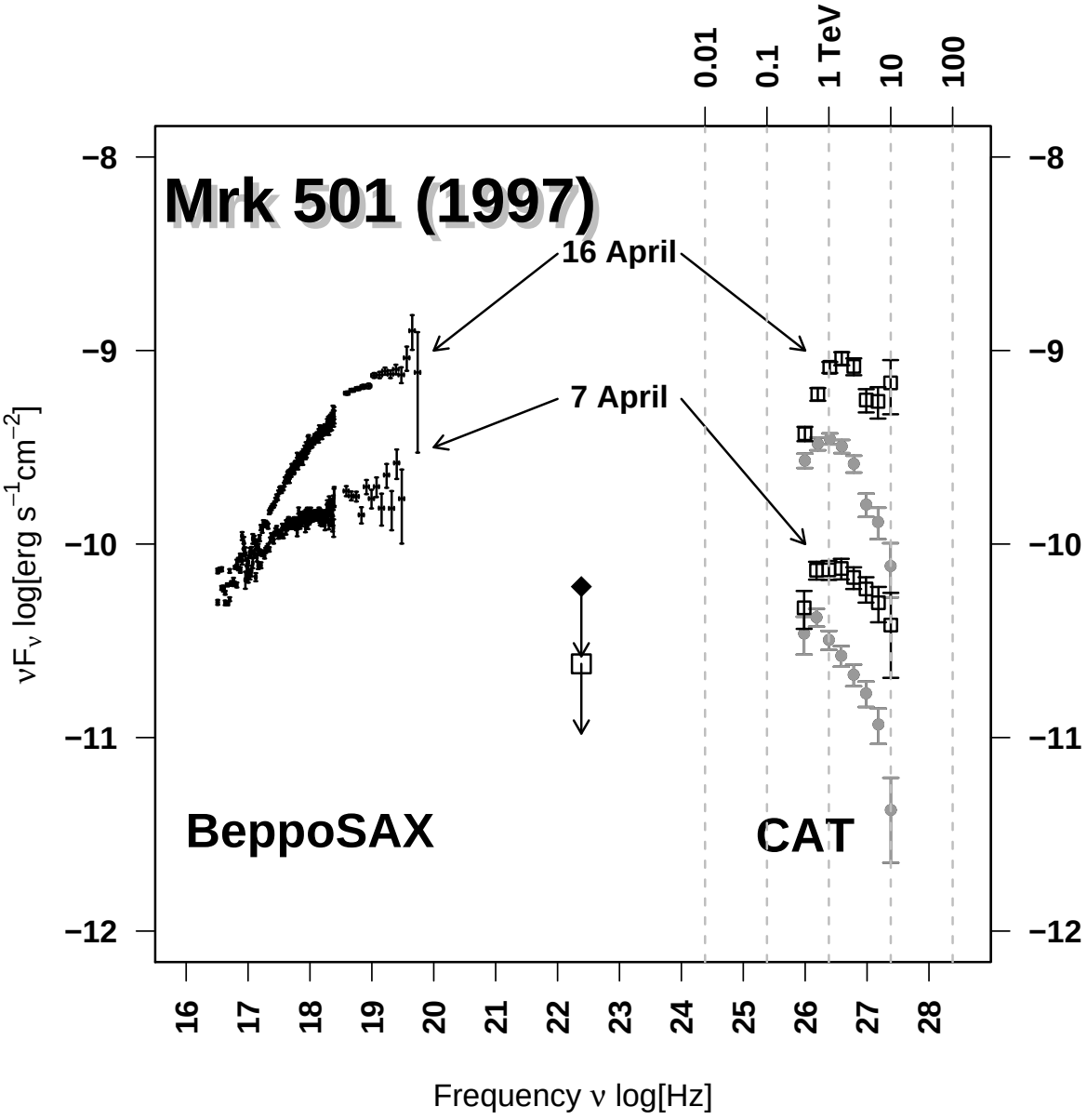

Fig. 2.— Spectral energy distribution of Mrk 501 during the flaring period in 1997 April, showing the simultaneous data taken by the Beppo-SAX instrument (Pian et al. 1998) and by the CAT imaging Atmospheric Čerenkov Telescope (Djannati-Ataï et al. 1999; Barrau et al. 1998). About high energy data points, filled gray circles are the CAT observed ones while open squares are unabsorbed ones, corrected from our estimation of the DIrB attenuation

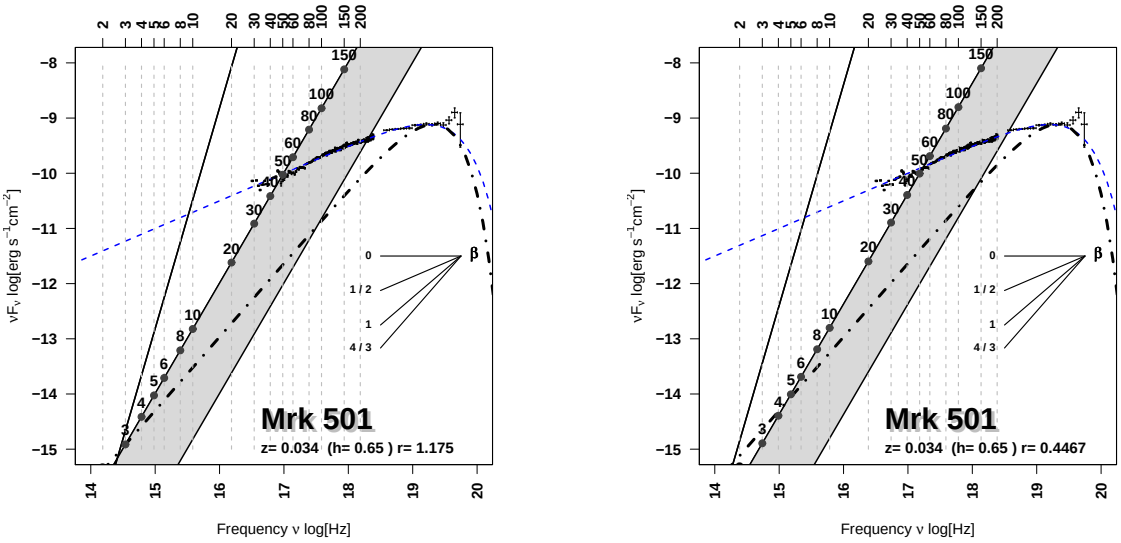

Fig. 3.— Constraints on the local shape of the synchrotron spectrum of Mrk 501 during the high 1997 April 16 high state. Grayed polygon is obtained considering the gamma transparency argument. It is defined by the zone where opacity lying into the interval $\tau_{\gamma\gamma} \times A^{1/2} \in [0.1, 1]$ where A is the aspect ratio. For an homogeneous spherical blob $A = 1$ while in the case of a jet $A = 1/\theta_j$ where θ_j is the characteristic opening angle of the jet. Constraint coming from the typical variability time scale leads to the most left straight thick line. Also represented in dotted-dashed line, a spectrum with a spectral index equals to 4/3 in νF_ν resulting from the emission of a (quasi-)monoenergetic distribution of electrons and/or positrons. Left (resp. right) pannel correspond to the de-reddened (resp. reddened) case.

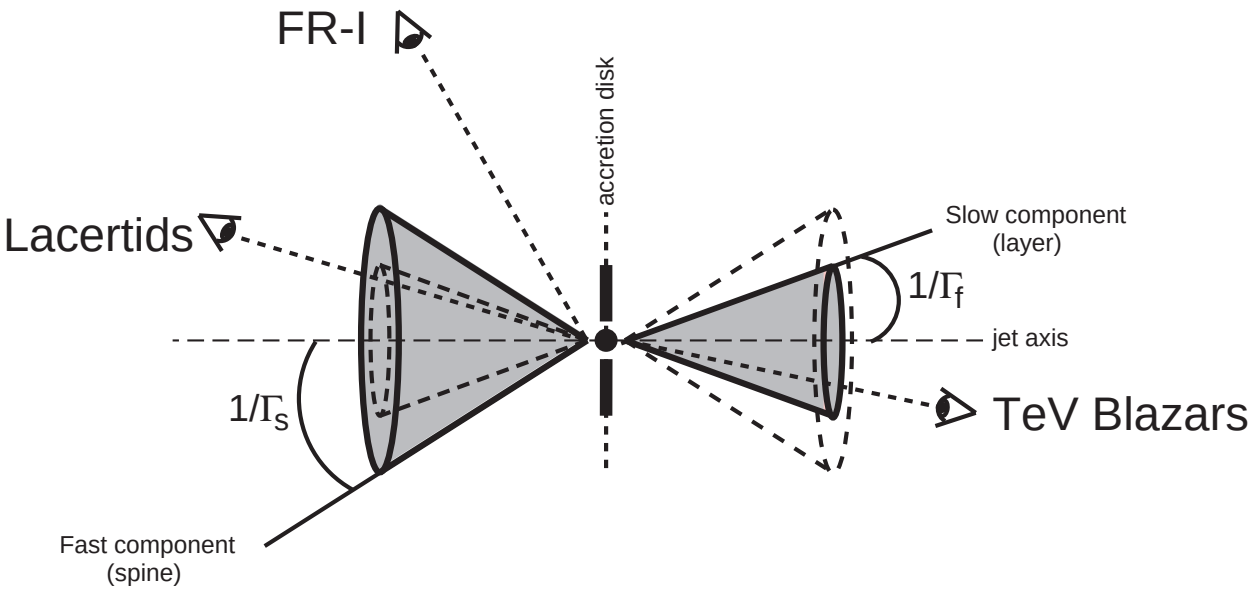

Fig. 4.— Sketch of the Two pattern model. It considers a relativistic external layer characterized by a Lorentz factor $\Gamma_{\rm s}$ and a fast internal spine with $\Gamma_{\rm s} > \Gamma_{\rm f}$. Considering relativistic Doppler beaming, an object viewed with $\theta > 1/\Gamma_{\rm s}$ refers to a FR-I radio galaxy. Conversely, if $\theta \leqslant 1/\Gamma_{\rm s}$ the source is seen as a BL Lac object and more precisely, if $\theta \leqslant 1/\Gamma_{\rm f}$ the fast inner component dominate the emission. In this latter case one deals with a TeV blazar.

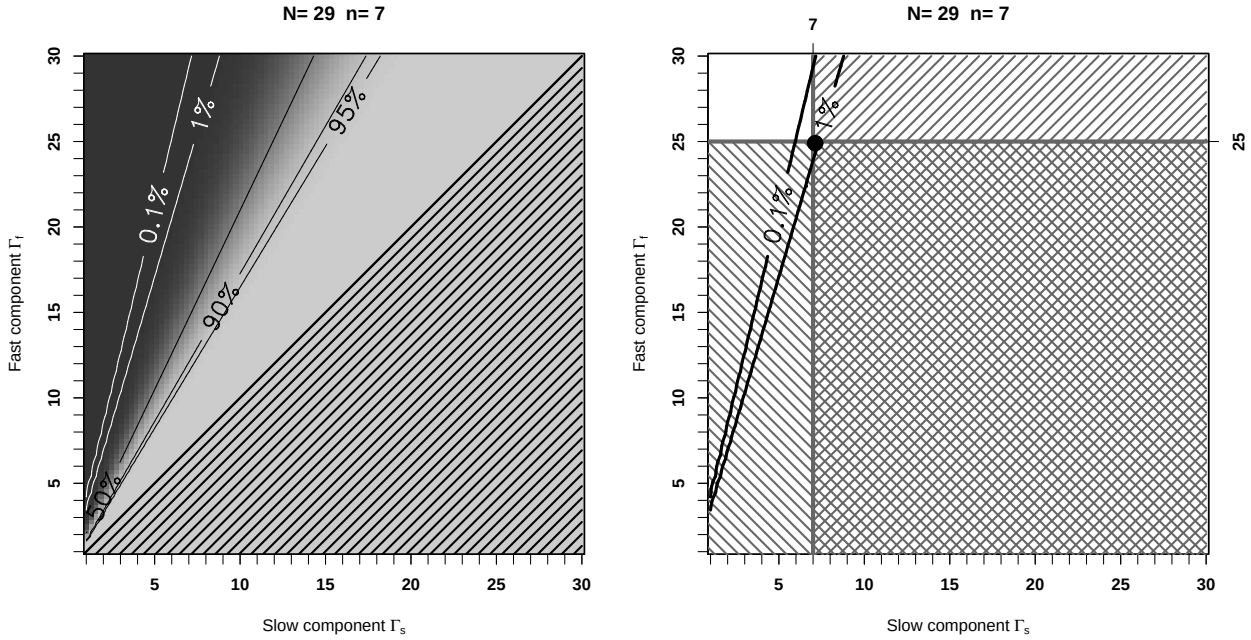

Fig. 5.— *Left panel.* Space parameters $(\Gamma_{\rm s}, \Gamma_{\rm f})$ constrained by the statistics of the number n of TeV blazars in a given population of N observed Lacertids. Each line corresponds equivelently to a constant value of $\mathcal{P}_0 = \mathcal{P}(29 \geqslant n_0 \geqslant 7)$ or of the ratio $\Gamma_{\rm s}/\Gamma_{\rm f}$. Here represented $\mathcal{P}_0 = 95\%, 90\%, 50\%, 1\%$ and 0.1% (see text for more details). *Right panel.* Same as previous panel but combined with the constraints coming from $\gamma-$rays transparency argument and FR-I/Lacertids unification models. The first one eliminates all the region lying above the $\Gamma_{\rm f,min} = 25$ while the seconde one suppress the right part of the parameters space $\Gamma_{\rm s} \geqslant \Gamma_{\rm s,max} = 7$. In this case, the allowed region compatible with a probability of detection of at least 7 TeV blazars in a population 29 Lacertids is strongly improbable.